Research Square

Preprints are preliminary reports that have not undergone peer review.
They should not be considered conclusive, used to inform clinical practice,
or referenced by the media as validated information.

IGF-2 Modified by the m^{6}A Demethylation Enzyme ALKBH5 in the Ossification of the Ligamentum Flavum

Ming-jie Kuang
Shandong Provincial Hospital
Hai-Feng Wang
Shandong Provincial Hospital
Jie Qiu
Shandong Provincial Hospital
An-bang Wang
Shandong Provincial Hospital
Feng Wang
Shandong Provincial Hospital
Bing-yi Tan
Shandong Provincial Hospital
Shi-jie Han
Shandong Provincial Hospital
Xiao-ming Li
Cangzhou People's Hospital
Da-Chuan Wang (wangdachaunsd@163.com)
Department of Orthopedics, The Provincial Hospital Affiliated to Shandong First Medical University, Jinan, Shandong 250014, China

Research

Keywords: RNA methylation, Ossification of the ligamentum flavu, m6A, IGF-2, ALKBH5

Posted Date: December 28th, 2020

DOI: https://doi.org/10.21203/rs.3.rs-130215/v1

License: This work is licensed under a Creative Commons Attribution 4.0 International License.
Read Full License

Abstract

Background: Ossification of the ligamentum flavum (OLF) is a pathological heterotopic ossification of the paravertebral ligament. However, the specific pathophysiology mechanism of this disease is still unknown. The m^6A methylation and its potential functions in OLF remain to be unexplored.

Method: In this study, we performed a transcriptome-wide methylation analysis using the OLF and normal ligaments to explore the mechanism of OLF. Common and region-specific methylation have different preferences for methylation site selection and thereby different impacts on their biological functions. We screened out the methylase-ALKBH5, and by promoting or inhibiting its expression, observing the content of m^6A, and measuring the ossification of ligaments, and then measuring IGF expression situation by alizarin red staining, alkaline phosphatase, immunofluorescence, immunohistochemistry, etc.

Result: MeRIP-seq and qPCR showed that the m6A methylation level of OLF group was usually higher than that of control group. In addition, we found that ALKBH5 is an important demethyltransferase in OLF, which promotes the expression of m^6A. ALKBH5 promotes the expression of IGF-2, which in turn promotes osteogenesis in OLF.

Conclusion: Overall, we provided a region-specific map of m^6A methylation and characterized the distinct features of specific and common methylation in OLF, and we proved that IGF-2 can be regulated by ALKBH5 to promote the process of OLF.

Introduction

Ossification of the ligamentum flavum (OLF) is a pathological heterotopic ossification of the paravertebral ligament that causes myelopathy[1]. OLF is a common spinal disorder with a high incidence in East Asian countries such as China, Korea and Japan[2]. As previously reported, the incidence of OLF is 20% over 65 years of age among elderly Japanese[3]. In a study of 1736 southern Chinese volunteers (1068 women and 668 men with mean 38 years of age) showed that the overall incidence of OLF is 8.3% in population, and 68.2% cases OLF was present at a single-level, whereas in 31.8% cases OLF was present at multiple levels[2]. Recently, several studies have reported that chronic pressure and genetic factors are the common cause for the development of OLF[4-6]. Since OLF only occured in limited areas of the world, genetic factors were considered as being more important in pathogenetic process. Several studies also strongly supported the view that OLF genetic component play an important role in OLF[1,2,7]. However, the specific pathophysiology mechanism of this disease is still unknown.

Application of gene analysis and molecular biology approaches were used to clarify etiology and pathology of OLF. Genes, for example, bone morphogenetic protein-2 (BMP2), transforming growth factor-beta 1(TGF-β1), and osteocalcin (OCN) related to osteogenic differentiation are believed to be associated with OLF[6,8]. Recently there have been intensively studies of epigenetic control of OPLL, and most studies focused on genetic polymorphisms and noncoding RNAs [9,10]. Yang et al reported that miR-490-3p was

found to be down-regulated during osteogenic differentiation of thoracic ligamentum flavum cells and miR-490-3p down-regulated the expression of FOXO1 and RUNX2 to inhibit the osteogenic differentiation of thoracic ligamentum flavum cells in OLF[10]. Han et al performed microarrays to investigate the differential expression of lncRNA, mRNA, circRNA between OLF tissues from OLF patients and normal tissue from healthy volunteers[11]. All these studies demonstrated that epigenetic modification played a key role in OLF.

RNA modifications such as N6-methyladenosine (m^6A), 5-methylcytidine (m^5C) and N1-methyladenosine(m^1A) have been proved to be essential regulatory elements in various biological processes[12-14]. m^6A was the most prevalent internal mRNA/lncRNA modifications in mammals[12]. Modification of m^6A depends on various methylated enzymes including methyltransferase-like 3 (METTL3), methyltransferase-like 14 (METTL14), wilms tumour 1-associated protein (WTAP) and KIAA1429 and demethylated enzymes including fat mass and obesity-associated protein (FTO)and alkB homologue 5 (ALKBH5)[15,16]. m^6A RNA modification was a dynamic process and its disturbance probably correlated to human diseases. Yang et al reported that linc1281 regulated mESC identity by sequestering pluripotency-related miR-let-7, and m^6A modification played an important role in this regulatory mechanism[14]. In addition, Liu et al showed that reduced m^6A methylation lead to decreased expression of negative AKT regulator PHLPP2 and increased the expression of positive AKT regulator mTORC2[17].

Recent studies have already shown that dysregulation of this m^6A modification may be associated with obesity, brain development abnormalities and cancers[18-20], thus emphasizing the importance of m^6A RNA modification. It was very important of m^6A in biological processes, but there were no studies that reported the role of m^6A in OLF. Here, we aim to explore the epigenetic alteration of m^6A in OLF. Study into the function of m^6A in osteogenic differentiation is necessary and might shed light on future clinical therapy and drug developments.

Materials And Methods

Clinical samples

OLF tissues were harvested from three OLF patients and normal ligamentum flavum tissues from three non-OLF patients who received surgery for spine trauma was harvested as a control. This study was approved by the institutional review board of the Provincial Hospital Affiliated to Shandong University, and all patients signed informed consent. Diagnosis of OLF was performed by professor Da-chuan Wang based on clinical symptoms and radiological examinations (including X-ray, computed tomography and magnetic resonance imaging) of the spine.

Cell culture and treatments

Cells from the ligamentum flavum tissues were cultured as previously reported[21].

Briefly, the ligament tissue was cut into small pieces under aseptic conditions and PBS

was used to wash the pieces three times to remove excess component. Next, 250 U/ml type 1A collagenase was used to digest the small pieces at 37°Cand shake every five minutes. After the small pieces are completely digested,stop the digestion process using Dulbecco's Modified Eagle's medium (DMEM) and 10% fetal bovine serum (FBS). Finally, the cells were cultured in six wells with DMEM containing 10% FBS with 100 U/ml of penicillin and 100 μg/ml of streptomycin at cell culture incubator.

Osteogenic differentiation assay and Alizarin red staining

As we previous reported, we prepared osteogenic differentiation medium as follows: α-MEM with 10% fetal bovine serum, 10 mM β-glycerophosphate, 10nM dexamethasone, and 50 μg/mL ascorbic acid [22]. Approximately 10^5 cells/well were were cultured in osteogenic differentiation medium. When the cells reached 60% confluence, the osteogenic differentiation medium was replaced with osteogenesis induction. After 21 days of induction, calci um mineral deposits were measured by Alizarin red staining using microscopy.

ALPstaining

ALP staining was used to evaluate the osteogenic effects as previously reported[23]. Approximately there were 10^5 cells/well in six well dishes. When the cells reached 60% confluence, the osteogenic differentiation medium was replaced with osteogenesis induction. After 7 days of induction, the induced cells were washed three times with PBS and then fixed with 4% formaldehyde for 20 minutes. An ALP staining solution was used to measure the ALP activity. After washing three times with PBS, the ALP activity was measured by microscopy.

Hematoxylin and Eosin (HE) staining assay

The HE staining was performed as we reported previously[24]. Briefly, the ossification ligament and normal ligament tissues were fixed in 4% paraformaldehyde at 4℃ for three days. Then the samples were embedded in paraffin and cut into 5-μm sections, deparaffinized in xylene, rehydrated through a series of graded ethanol, and washed in distilled water. Hematoxylin and Eosin (HE) staining was performed for histological observation.

Immunohistochemical (IHC) staining assay

In addition, IHC staining was used to evaluate the osteogenesis effect and the expression of IGF-2. The ossification ligament and normal ligament tissues were fixed in 4% paraformaldehyde at 4°C for three days. Then the samples were embedded in paraffin and cut into 5-μm sections,deparaffinized in xylene, rehydrated through a series of graded ethanol, and washed in distilled water. Subsequently, 3% hydrogen peroxide was used as a catalase quencher, and then the tissue sections were blocked in 10% goat serum (Sigma-Aldrich) for 1 hour. After washing with PBS for three times, an anti-IGF-2 antibody (1:100; Abcam;

Cat. no. ab9574) was incubated with the sections at 4°C overnight, with non-immune serum as a control. Next, the tissue sections were incubated with a biotin-labeled secondary antibody (1:100; Proteintech; Cat. no. SA00004-6), and the signal was amplified and visualized with the chromogen diaminobenzidine, followed by hematoxylin counterstaining.

Immunofluorescent staining

The samples of OLF and normal ligamentum flavum tissues were obtained and cut into 5-μm sections. And then the sections were fixed at 4°C for 20 min. The sections were incubated with the anti-IGF-2 antibody (1:100; Abcam; Cat. no. ab9574) and anti-ALKBH5 (1:1000; Abcam; Cat. no. ab195377) antibody at 37°C for 2 hours. The fluorescently-labeled antibody was used to incubate with the sections at dark for 1 hour. After washed with three times, the sections were imaged using confocal microscope.

Vector construction and transfection

The human lentivirus-si-ALKBH5 (si-ALKBH5) and lentivirus-ALKBH5 (lv-ALKBH5) were purchased from Sangon Biotech (Shanghai, China). Puromycin was used to select the transfected cells for 7 days. The surviving cells were used as stable mass transfectants to perform the subsequent assays.

Dual Luciferase reporter assay

PCR product containing 300bp of the 3'-UTR of IGF-2 (wild-type and mutant) was first inserted into pGL3-basic vector. Then 200 ng pGL3-IGF-2(wild-type and mutant) promoter, along with 40 ng pRL-TK Vector (E2241, Promoga) were respectively transfected into the cells with over-expressed ALKBH5 or negative control using Lipofectamine 2000. The luciferase reporter assays were performed 48 hours after transfection using the Dual Luciferase Reporter Assay System (E1910, Promega).

Western blotting assay

Protein from the specimens were extracted using lysis buffer, and 20 ug of proteins was loaded into 10% SDS–PAGE gel and transferred to PVDF membranes (Millipore, Bedford, MA, USA). After blocking with 5% skimmed milk, the PVDF membranes were incubated with primary antibody including anti-ALKBH5 (1:1000; Abcam; Cat. no. ab195377), anti-IGF-2 antibody (1:1000; Abcam; Cat. no. ab9574) and GAPDH (1:1000; Abcam; Cat. no.ab9485) at 4℃ overnight. Next, the PVDF membranes were incubated with secondary antibody conjugated-horseradish peroxidase (1:1000; Proteintech; Cat. SA00001-2), and the bands were visualized using ECL detection reagents (Millipore).

Real-Time reverse transcriptase polymerase chain reaction

Real-time reverse transcriptase polymerase chain reaction (RT-PCR) was performed as we previously reported[22]. Trizol reagent (Invitrogen) was used to extract total RNA. PrimeScript RT reagent kit (TaKaRa, Japan) was used for reverse transcription. Real-time PCR analysis was performed using the SYBR Premix

Ex Taq II kit (TaKaRa) and detected on the Roche LightCycler 480 sequence detection system. GAPDH were used as loading control for quantitation of mRNA.

Methylated RNA Immunoprecipitation and high-throughput RNA sequencing (MeRIP-seq)

MeRIP-Seq was performed by Cloudseq Biotech Inc. (Shanghai, China) according to the published procedure which was slight modifications. Briefly, the fragmented RNA was incubated with m^6A polyclonal antibody (Synaptic Systems, 202003) in IPP buffer at 4°C for 2 hours. Then the mixture was immune-precipitated by incubation with protein-A beads (Thermo Fisher) at 4°C for an additional 2 hours. Then, bound RNA was eluted from the beads with N6-methyladenosine (BERRY & ASSOCIATES, PR3732) in IPP buffer and then extracted with Trizol reagent (Thermo Fisher) by following the manufacturer's instruction. Purified RNA was used for RNA-seq library generation with NEBNext® Ultra™ RNA Library Prep Kit (NEB). Both the input sample without immunoprecipitation and the m^6A IP samples were subjected to 150 bp paired-end sequencing on Illumina HiSeq sequencer. In addition, the q-PCR was performed to detect the level of m^6A using purified RNA fragments.

Data of MeRIP-seq processing and bioinformatics analysis

Paired reads were harvested from Illumina HiSeq 4000 sequencer, and were quality controlled by Q30. After 3' adaptor-trimming and low quality reads removing by cut adapt software (v1.9.3). First, clean reads of all libraries were aligned to the reference genome (UCSC HG19) by Hisat2 software (v2.0.4). ExomePeak software was used for identifying RNA m^6A-modified regions (m^6A peaks) with FDR (false discovery rate) < 0.05. As previously reported[25], the common methylated RNAs (CMRs) were defined as RNAs containing at least one m^6A peak in all samples, while the specific methylated RNAs (SMRs) were the RNAs with m^6A modification only in one sample, and m6A peaks of SMRs were defined as specific m^6A peaks. Biological process, molecular function and cellular component analysis were performed for the enrichment of differentially methylated genes, CMRs and SMRs.

Statistical analysis

All these experiments were repeated at least three times. The data were shown as means ± standard deviation (SD). Means of multiple groups were compared by one-way analysis of variance (with Fisher's least significant difference [LSD] test). Statistical analysis was conducted in SPSS 20.0 software (IBM Corp., Armonk, NY, USA). Data with *P* values <0.05 was considered statistically significant.

Results

The identification of OLF and ubiquitous expression of m^6A writers and erasers in the OPLL and Control tissues

The CT and MRI was used to evaluate the level of ossification in the ligamentum flavu (**Fig1.A**). In addition, the HE staining was performed to evaluate the morphology between the tissues obtained from

the OLF patients and patients with fractures. And the results showed that the tissue in OLF patients have been replaced by bone tissues and the tissue in control group was fibrous connective tissue (**Fig1.B**). Next, to gain insight into the m^6A RNA methylation profiles in the OLF and control tissues, MeRIP-seq was performed to detect the methylation between the OLF and control group. The results of input were showed by venn diagram and 327 genes were found among three samples in control group (**Fig1.C**), and 695 genes were found among three samples in OLF group (**Fig1.D**). In addition, the differential expressed genes between the control and OLF group were also detected and the results showed that 268 genes were down regulated in control group and 77 genes were up regulated in OLF group (**Fig1.E**). Also, the level of methylation between control and OLF group was also investigated, and the results showed that 169 common peaks and 79 specific peaks were found in OLF group and 169 common peaks and 272 specific peaks were found in control group indicating that RNA methylation constitutes an additional layer of regulation in a region-specific manner (**Fig1.F**). Fold enrichment of peaks and genes between two groups were also calculated with log2 standardization. There was significant difference between OLF and control group in peaks (**Fig1.G**) and genes (**Fig1.H**). Taken together, this comparative analysis revealed that the methylation levels in OLF were lower than those of control group.

Different distribution patterns between common and specific m^6A peaks

To detect the m^6A methylation specific consensus sequences and enrichment sites in the OLF and control group, motif-searching analysis were performed with all m^6A peaks and the results showed that GCACGUCGUAACGUACU /CAACUGACGUCGUAACG were the most conserved consensus motifs between the OLF and control group (**Fig. 2A**). The distribution patterns of all m^6A peaks along the transcript from 5'UTR to 3'UTR were detected. The results showed that a pronounced enrichment was found surrounding from 5'UTR to 3'UTR in both the OLF and control group. And there was significant difference in the 5'UTR and 3'UTR region between the OLF and control group, but no significant difference was found in CDS region (**Fig. 2B**). Next, common m^6A peaks was also evaluated, and the results showed that pronounced enrichment from 5'UTR to 3'UTR, however, there was no significant difference between the OLF and control group (**Fig. 2C**). And significant difference was found in 5'UTR and 3'UTR region for specific peaks (**Fig. 2D**). Due to the significant difference in specific peaks from 5'UTR to 3'UTR, we investigated the distribution patterns of specific peaks in detail. And the peak numbers enriched in each gene region between the OLF and control group (**Fig. 2E**). When taking all the methylation sites into consideration, m^6A sites near the 5'UTR and start codons were the most abundant (**Fig. 2F**). Notably, genes and distribution patterns of m^6A were analyzed using CMR and SMR. The results showed that significant difference was found between the OLF-specific CMR and SMR in genes and distribution patterns of m^6A, and there was significant difference between the control-specific CMR and SMR genes and distribution patterns of m^6A (**Fig. 2F and 2G**). CMRs and SMRs differed from each other in their methylation levels and overall m^6A abundance, suggesting that common and specific methylation regulate gene expression in different ways.

The m^6Ademethylase ALKBH5 regulated osteogenesis in OLF

We firstly evaluated the global m^{6}A level in samples of OLF and control patients, and the results revealed that the m^{6}A methylation decreased in OLF group (**Fig. 3A**). As previously reported, ALKBH5 played an important role in regulating cell functions[26]. Therefore, we evaluated the expression of ALKBH5 in OLF and control group at first, and the results showed that ALKBH was upregulated in OLF group (**Fig. 3B**). The results of western blotting also verified that ALKBH5 was upregulated in OLF group (**Fig. 3C and 3D**). The transfection efficiency was evaluated using western blotting and the results showed that the ALKBH5 can be inhibited or overexpressed effectively in si-ALKBH5 or lv-ALKBH5 group (**Fig. 3E**). To explore the osteogenesis effect of ALKBH5 in OLF, the ALKBH5 was inhibited or overexpressed and evaluated using alizarin red staining in normal ligamentum flavum cells. The results revealed that overexpressed the ALKBH5 can promote the osteogenesis and the osteogenesis effect was inhibited when down regulated the ALKBH5 (**Fig. 3F and 3G**). Therefore, the ALKBH5 play an important role in osteogenesis in OLF.

Distinct biological functions of commonly and specifically methylated genes

We conducted GO analysis to explore the biological relevance of common and specific methylation in the OLF and control group. The top 4000 m^{6}A peaks containing CMRs were selected for GO analysis. These CMRs were enriched in very similar categories including skeletal system development, negative regulation of cellular process, and post-embryonic development suggesting that m^{6}A was an essential modification involved in diverse physiological processes (**Fig. 4A**). The GO cellular component classification of CMRs revealed that membrane-bounded organelle and extra-cellular region was the most abundant part (**Fig. 4B**). The molecular function of CMRs was also estimated using enrichment score, and the results showed that insulin-like growth factor receptor binding played an important role in m^{6}A modification (**Fig. 4C**). The GO cellular component classification of SMRs revealed that nucleus and nucleoplasm was the most abundant part (**Fig. 4D**). Also negative regulation of execution phase of apoptosis, regulation of RNA metabolic process and stem cell proliferation was the most important function in SMRs of m^{6}A modification (**Fig. 4E and 4F**).

IGF-2 was regulated by m^{6}Ademethylase ALKBH5 in OLF

MeRIP was performed to investigate the function of ALKBH5 that can promote osteogenesis. The results showed that the m^{6}A methylation of IGF-2 in NC-IP group was significantly increased when compared with the OLF-IP group, which indicated that IGF-2 was regulated by m^{6}A methylation modification (**Fig. 5A**). Also, the MeRIP-q-PCR was performed to evaluate the m^{6}A methylation in OLF and control group. The results showed that the m^{6}A methylation in OLF group was significantly decreased compared with control group (**Fig. 5B**). We also detected the level of m^{6}A methylation in normal cells and the results showed that the m^{6}A methylation of IGF-1 was significantly increased (**Fig. 5C**). Next, we over-expressed the ALKBH5 and the m^{6}A methylation of IGF-2 was evaluated using MeRIP-qPCR, and the results showed that over-express ALKBH5 can decrease the level of m^{6}A methylation when compared with the control group (**Fig. 5E**). Also, when over-expressed the ALKBH5, the expression of IGF-2 was increased. The expression of IGF-2 decreased when the ALKBH5 was inhibited (**Fig. 5F**). The stability of IGF-2 mRNA was

also detected using ActD assay, and the result showed that there was significant difference between the over-expressed ALKBH5 and control group at 4 and 6 hours (**Fig. 5G**). The luciferase reporter assay showed that no significant difference was found when the adenosine site was mutated between the lv-ALKBH5 and control group. However, significant difference was observed in wide-type of IGF-2 product between the lv-ALKBH5 and control group (**Fig. 5H**). The immunofluorescent staining was used to detect expression of IGF-2, and the results showed that over-expressed ALKBH5 can promote the expression of IGF-2 when compared with the control group (**Fig. 5I**).

m^6Ademethylase ALKBH5 regulated osteogenesis through IGF-2 demethylation

Alizarin red staining and ALP staining were used to evaluate the osteogenesis effect. The results showed that the osteogenesis ability decreased when the IGF-2 was inhibited. Over-expressed ALKBH5 can reverse the effect caused by si-IGF-2 (**Fig.6A**). And over-expressed IGF-2 can promote the osteogensis when compared with the control group (**Fig.6A**). Also the samples of OLF or control group was sectioned and stained using ALKBH5 and IGF-2 anti-bodies. The results showed that the expression of ALKBH5 and IGF-2 was significantly increased in OLF group when compared with the control group (**Fig.6B**). We also performed IHC staining to evaluate the expression of ALKBH5 and IGF-2. The results showed that ALKBH5 and IGF-2 was over-expressed in OLF tissue when compared with the control group (**Fig.6C**). All these data suggested that the IGF-2 was regulated by ALKBH5 to regulate osteogenesis in OLF.

Discussion

OLF was a condition that is characterized by the heterotopic ossification in ligamentum flavum. Although the underlying pathogenesis was currently unclear, previously studies have reported that OLF was influenced by several different genetic and environmental factors[3,27]. In this study, we performed the first region-specific m^6A RNA methylation map to explore the potential mechanism of OLF. And we verified that ALKBH5 played an important role in OLF by targeting IGF-2 m^6A demethylation.

RNA served as an inevitable connecting link for genetic information passing from DNA to protein. Post-transcriptional mRNA regulation played an important role in cellular function regulation. m^6A was the most ample RNA modification in eukaryotic mRNA[17]. Recently, more and more studied focused on the m^6A methylation in the regulation of mRNA stability, splicing, and translation [15,17]. As previously reported, Chen et al found that METTL3 was significantly up-regulated in human hepatocellular carcinoma and knockdown of METTL3 can reduce the SOCS2 mRNA m^6A modification and promoted SOCS2 mRNA expression to reduce human hepatocellular carcinoma cell proliferation, migration and colony formation[19]. Liu et al reported that METTL14 mutation or reduced the expression of METTL3 can increase the endometrial cancer cells proliferation and tumorigenicity through AKT signaling pathway activation[17]. In our study, MeRIP-seq was performed to investigated the related genes with m^6A modification. And the OLF group contained less methylated RNAs with lower methylation levels when compared with the control group. m^6A methylation was a fundamental requirement for CMRs to exert

their functions in various physiological processes, but specific methylation is only needed on specified occasions[25]. Therefore, the methylation levels of CMRs were higher than those of SMRs significantly. We found that the RNA methylation level in the OLF group was lower than control group.

The m^6A methylation regulated the cellular function mainly through the methyhransferases including METTL3, METTL14, ALKBH5 and so on[12]. Previously studies have verified that ALKBH5 can regulate the target mRNA demethylation to affect the cellular processes[20,26]. Li et al[26] reported that ALKBH5 promoted trophoblast invasion at the maternal-fetal interface by regulating the stability of CYR61. In our study, we showed that ALKBH5 was up-regulated in OLF group compared with the control group, and ALKBH5 can promote osteogenesis in OLF. Moreover, multiple lines of data including osteogenesis assay, cell proliferation assay and clinical samples analysis in this study have verified that ALKBH5 mediated osteogensis via IGF-2 expression. Therefore, all these data suggesting ALKBH5 can play an important role in OLF through IGF-2 demethylation. Previously studied have reported that IGF-2 showed the osteogenesis effect to promote bone regeneration.

Conclusion

In this study, our results revealed several novel insights regarding the mechanism of m^6A methylation in the OLF. Firstly, m^6A methylation levels in normal tissues are generally higher than the OLF tissue. Secondly, heterogeneity of RNA methylation exists, including the RNAs that are methylated, their methylation levels and the methylation sites. And common and region-specific methylation have different preferences for methylation site selection and thereby different impacts on their biological functions. Thirdly, we firstly reported the AKLBH5 play an important role in osteogenesis to regulate OLF. Lastly, our results verified that IGF-2 was regulated by ALKBH5 to promote osteogenesis in OLF. Therapeutic methods that target ALKBH5 and IGF-2 may be effective for the treatment of OLF.

Abbreviations

OLF: Ossification of the ligamentum flavu

IGF-2: Insulin-like growth factor 2

m^6A: N6-methyladenosine

MeRIP-seq: Methylated RNA Immunoprecipitation and high-throughput RNA sequencing

qPCR: quantitative real time polymerase chain reaction

BMP2: Qbone morphogenetic protein-2

TGF-β1: Transforming growth factor-beta 1

OCN: Osteocalcin

OPLL: oOsification of the posterior longitudinal ligament

FOXO1: Forkhead box O1

RUNX2: Runt-related transcription factor 2

m^5C : N5-methylcytidine

m^1A: N1-methyladenosine

METTL3: Methyltransferase-like 3

METTL14: Methyltransferase-like 14

WTAP: Wilms tumour 1-associated protein

FTO: Fat mass and obesity-associated protein

ALKBH5: AlkB homologue 5

mESC: Mouse embryonic stem cells

PHLPP2: PH domain and leucine rich repeat protein phosphatase 2

Mtor: Mechanistic target of rapamycin

DMEM: Dulbecco's Modified Eagle's medium

FBS: Fetal bovine serum

α-MEM: α-minimum essential medium

ALP: Alkaline phosphatase

HE: Hematoxylin and Eosin

IHC: Immunohistochemical

lv-ALKBH5: Lentivirus-ALKBH5

si-ALKBH5: Lentivirus-si-ALKBH5

PCR: Polymerase chain reaction

RT-PCR: Real-Time reverse transcriptase polymerase chain reaction

GAPDH: Glyceraldehyde-3-phoshate dehydrogenase

CMRs: Common methylated RNAs

SMRs: Specific methylated RNAs

SD: Standard deviation

LSD: Least significant difference

Declarations

Conflict of interest

The authors declare no conflict of interest.

References

1. Takahashi T, Hanakita J, Minami M. Pathophysiology of Calcification and Ossification of the Ligamentum Flavum in the Cervical Spine. *Neurosurgery clinics of North America.* 2018;29(1):47-54.
2. Guo JJ, Luk KD, Karppinen J, Yang H, Cheung KM. Prevalence, distribution, and morphology of ossification of the ligamentum flavum: a population study of one thousand seven hundred thirty-six magnetic resonance imaging scans. *Spine.* 2010;35(1):51-56.
3. Miyasaka K, Kaneda K, Sato S, et al. Myelopathy due to ossification or calcification of the ligamentum flavum: radiologic and histologic evaluations. *AJNR. American journal of neuroradiology.* 1983;4(3):629-632.
4. Ono K, Yonenobu K, Miyamoto S, Okada K. Pathology of ossification of the posterior longitudinal ligament and ligamentum flavum. *Clin Orthop Relat Res.* 1999(359):18-26.
5. Furusawa N, Baba H, Imura S, Fukuda M. Characteristics and mechanism of the ossification of posterior longitudinal ligament in the tip-toe walking Yoshimura (twy) mouse. *European journal of histochemistry : EJH.* 1996;40(3):199-210.
6. Yayama T, Mori K, Okumura N, et al. Wnt signaling pathway correlates with ossification of the spinal ligament: A microRNA array and immunohistochemical study. *Journal of orthopaedic science : official journal of the Japanese Orthopaedic Association.* 2018;23(1):26-31.
7. Ohara Y. Ossification of the Ligaments in the Cervical Spine, Including Ossification of the Anterior Longitudinal Ligament, Ossification of the Posterior Longitudinal Ligament, and Ossification of the Ligamentum Flavum. *Neurosurgery clinics of North America.* 2018;29(1):63-68.
8. Kim HN, Min WK, Jeong JH, et al. Combination of Runx2 and BMP2 increases conversion of human ligamentum flavum cells into osteoblastic cells. *BMB reports.* 2011;44(7):446-451.
9. Uchida K, Baba H, Maezawa Y, et al. Increased expression of neurotrophins and their receptors in the mechanically compressed spinal cord of the spinal hyperostotic mouse (twy/twy). *Acta neuropathologica.* 2003;106(1):29-36.

10. Yang X, Qu X, Meng X, et al. MiR-490-3p inhibits osteogenic differentiation in thoracic ligamentum flavum cells by targeting FOXO1. *Int J Biol Sci.* 2018;14(11):1457-1465.
11. Han Y, Hong Y, Li L, et al. A Transcriptome-Level Study Identifies Changing Expression Profiles for Ossification of the Ligamentum Flavum of the Spine. *Molecular therapy. Nucleic acids.* 2018;12:872-883.
12. Zhao BS, Roundtree IA, He C. Post-transcriptional gene regulation by mRNA modifications. *Nature reviews. Molecular cell biology.* 2017;18(1):31-42.
13. Fu Y, Dominissini D, Rechavi G, He C. Gene expression regulation mediated through reversible mâ¶A RNA methylation. *Nature Reviews Genetics.* 2014;15(5):293-306.
14. Yang D, Qiao J, Wang G, et al. N6-Methyladenosine modification of lincRNA 1281 is critically required for mESC differentiation potential. *Nucleic acids research.* 2018;46(8):3906-3920.
15. Frye M, Harada BT. RNA modifications modulate gene expression during development. 2018;361(6409):1346-1349.
16. Panneerdoss S, Eedunuri VK, Yadav P, et al. Cross-talk among writers, readers, and erasers of m(6)A regulates cancer growth and progression. 2018;4(10):eaar8263.
17. Liu J, Eckert MA. m(6)A mRNA methylation regulates AKT activity to promote the proliferation and tumorigenicity of endometrial cancer. 2018;20(9):1074-1083.
18. Amort T, Rieder D, Wille A, et al. Distinct 5-methylcytosine profiles in poly(A) RNA from mouse embryonic stem cells and brain. 2017;18(1):1.
19. Chen M, Wei L, Law CT, et al. RNA N6-methyladenosine methyltransferase METTL3 promotes liver cancer progression through YTHDF2 dependent post-transcriptional silencing of SOCS2. 2017.
20. He Y, Hu H, Wang Y, et al. ALKBH5 Inhibits Pancreatic Cancer Motility by Decreasing Long Non-Coding RNA KCNK15-AS1 Methylation. *Cellular physiology and biochemistry : international journal of experimental cellular physiology, biochemistry, and pharmacology.* 2018;48(2):838-846.
21. Zhong ZM, Chen JT. Phenotypic characterization of ligamentum flavum cells from patients with ossification of ligamentum flavum. *Yonsei medical journal.* 2009;50(3):375-379.
22. Kuang M-j, Zhang W-h, He W-w, et al. Naringin regulates bone metabolism in glucocorticoid-induced osteonecrosis of the femoral head via the Akt/Bad signal cascades. *Chemico-biological interactions.* 2019;304:97-105.
23. Georges R, Béatrice V, Fred D, Roland B, Sergio RR. BMP-2 controls alkaline phosphatase expression and osteoblast mineralization by a Wnt autocrine loop. *Journal of Bone & Mineral Research.* 2010;18(10):1842-1853.
24. Kuang MJ, Xing F, Wang D, Sun L, Ma JX, Ma XL. CircUSP45 inhibited osteogenesis in glucocorticoid-induced osteonecrosis of femoral head by sponging miR-127-5p through PTEN/AKT signal pathway: Experimental studies. *Biochemical and biophysical research communications.* 2019;509(1):255-261.
25. Ma C, Chang M, Lv H, et al. RNA m(6)A methylation participates in regulation of postnatal development of the mouse cerebellum. 2018;19(1):68.

26. Li XC, Jin F, Wang BY, Yin XJ, Hong W, Tian FJ. The m^6A demethylase ALKBH5 controls trophoblast invasion at the maternal-fetal interface by regulating the stability of CYR61 mRNA. *Theranostics.* 2019;9(13):3853-3865.
27. Nouri A, Tetreault L, Singh A, Karadimas SK, Fehlings MG. Degenerative Cervical Myelopathy: Epidemiology, Genetics, and Pathogenesis. *Spine.* 2015;40(12):E675-693.

Figures

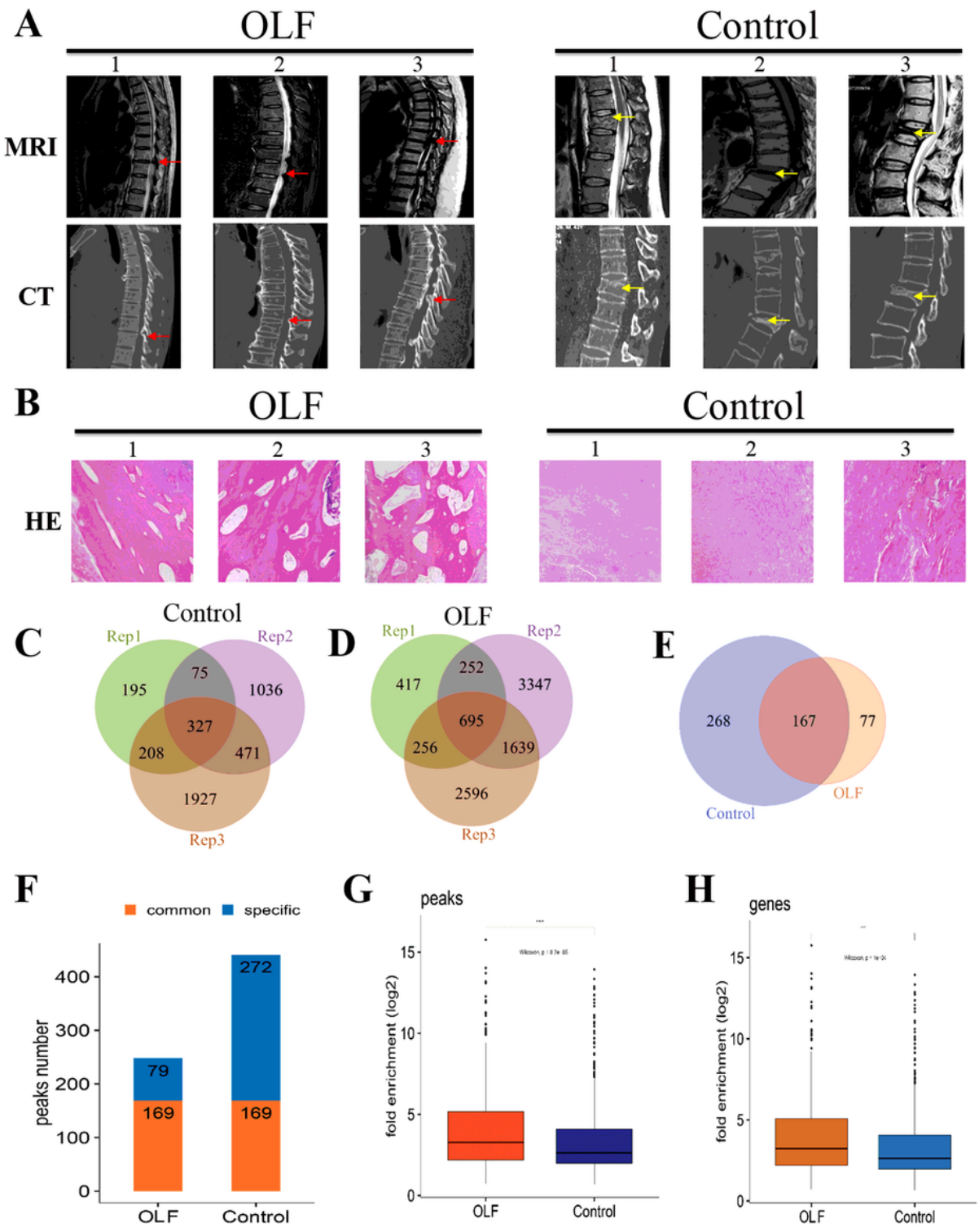

Figure 1

The identification of OLF and control tissues in morphology and m6A methylation. (A) The MRI and CT scan of OLF and fracture patients to identify the ossification of ligamentum flavum. (B) The HE staining was performed to detect the morphology of OLF and normal ligamentum flavum. (C, D) Venn diagrams was conducted to identify the numbers of overlapping m6A transcripts in the two biological replicates of m6A-IP the control and the OLF groups. (E) Venn diagram showing the numbers of CMRs and SMRs

between the OLF and control group. (F) Column chart showed the numbers of common and specific m6A peaks between the OLF and control groups. The blue bars indicated common peaks, while the orange bars indicated specific peaks. (G, H) Box plots was conducted to present the methylation levels of OLF RNAs and non-OLF RNAs by comparing the median fold enrichment at peak levels (G) and gene levels (H).

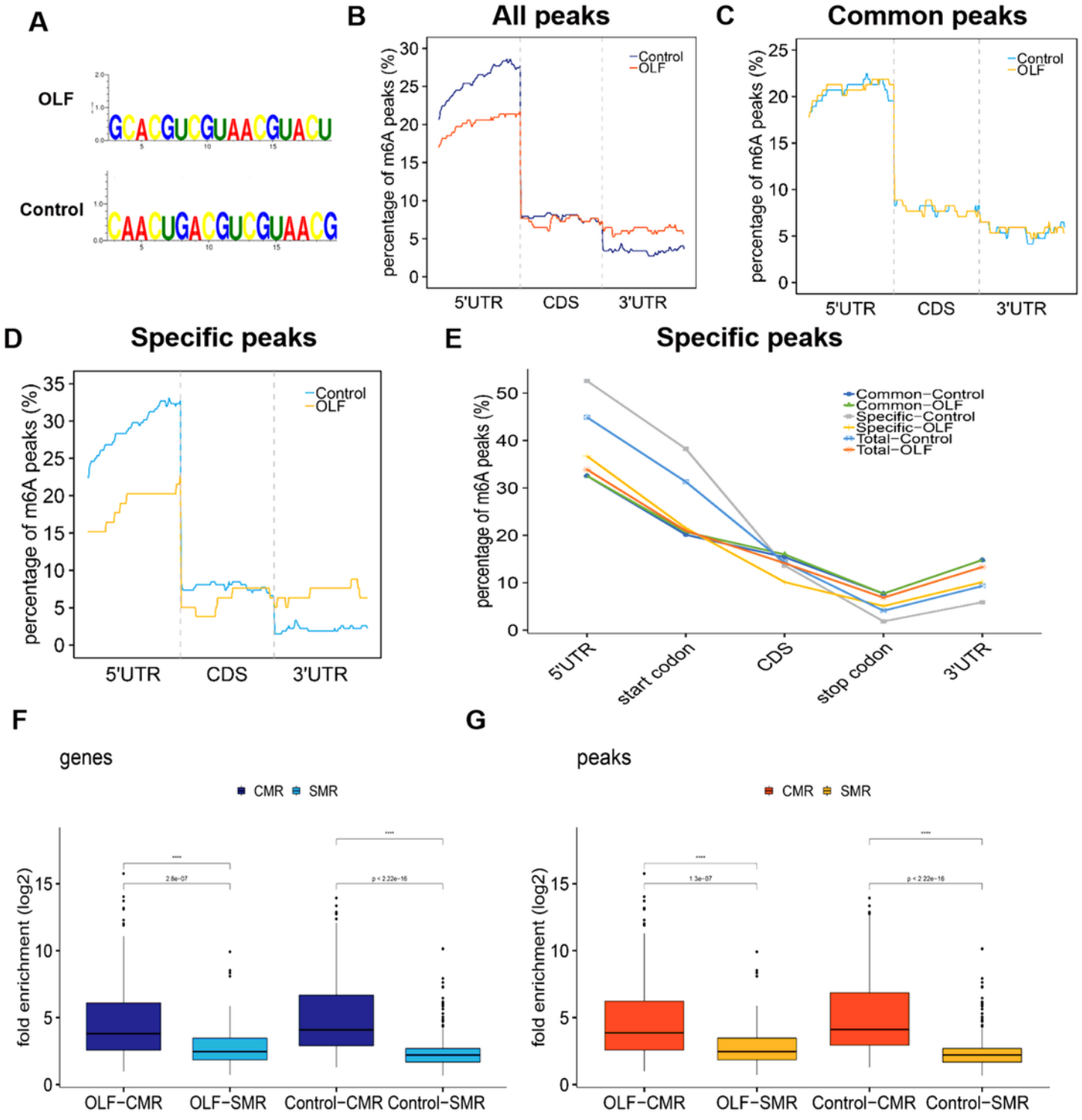

Figure 2

Distribution patterns of m6A peaks between the OLF and control group were detected using MeRIP-seq. (A) Sequence logo representing the deduced consensus motif through clustering of all enriched m6A peaks between OLF and control group. (B–D) Enrichment of all m6A peaks (B), common m6A peaks (C) and specific m6A peaks (D) along the whole mRNA transcripts. (E) The percentage of specific m6A peaks along the 5'UTR, start codon, CDS, stop codon and 3'UTR between common-control group, common-OLF group, specific-control group, specific-OLF group and total-OLF. (F, G) Box plots was conducted to detect the methylation levels of CMRs and SMRs by comparing the fold enrichment at the gene level (F) or peaks level (G). Wilcoxon test was performed for statistical analysis. *** p value<0.001.

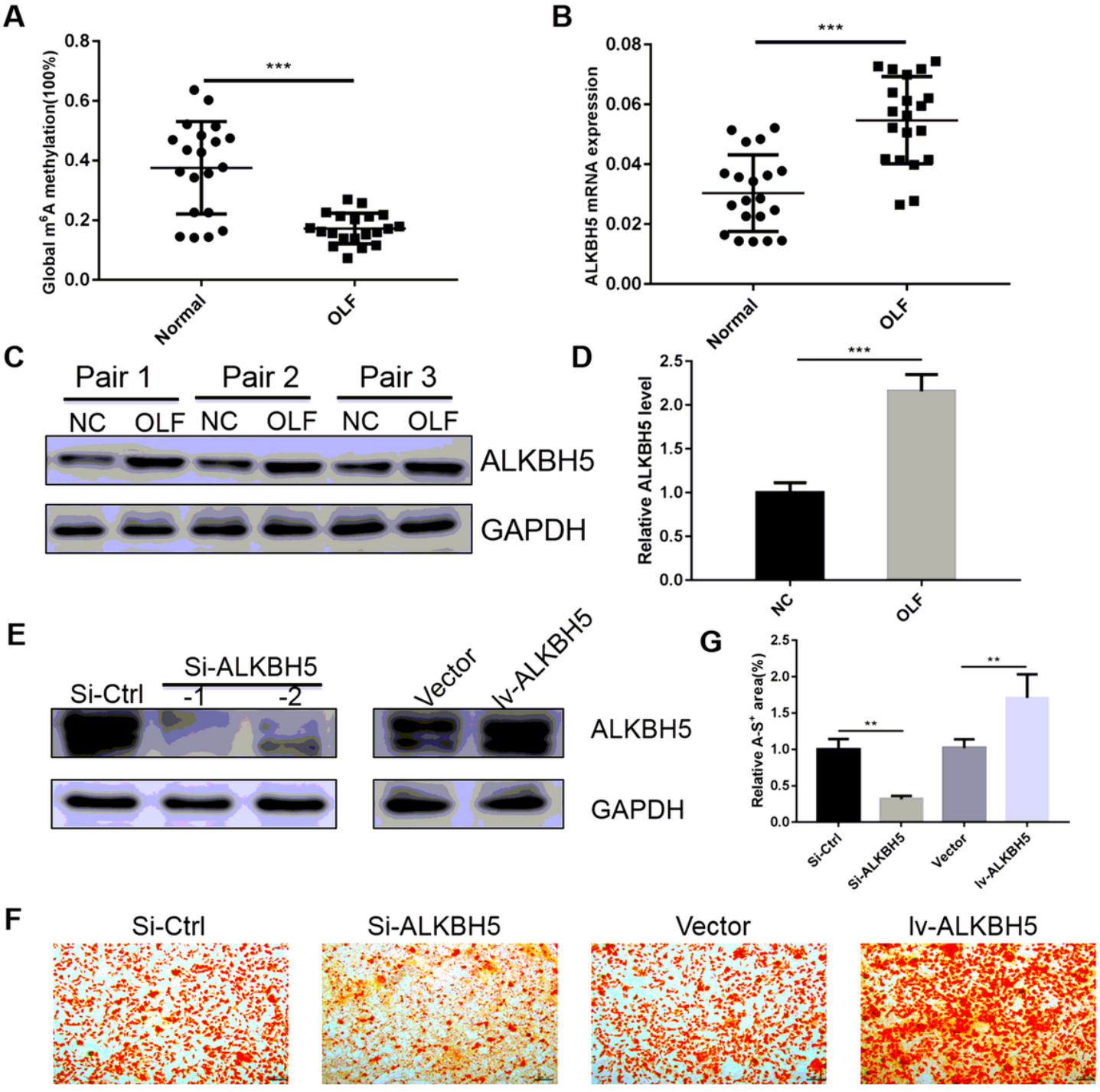

Figure 3

The m6A methylation was detected in OLF or control groups. (A) The global of m6A methylation was detected between OLF and normal group. (B) The expression of ALKBH5 was detected using q-PCR between OLF and normal groups. (C) Western blotting was performed to verify the expression of ALKBH5 in three pairs of tissues. (D) The quantitative calculation of western blotting using Image J software. (E) The transfection efficiency of knock down and overexpression of ALKBH5 was evaluated using western blotting. (F) The alizarin red staining was performed to investigate the osteogenesis when transfected with si-ALKBH5 or lvALKBH5. (G) The quantitative calculation of alizarin red staining using Image J software.

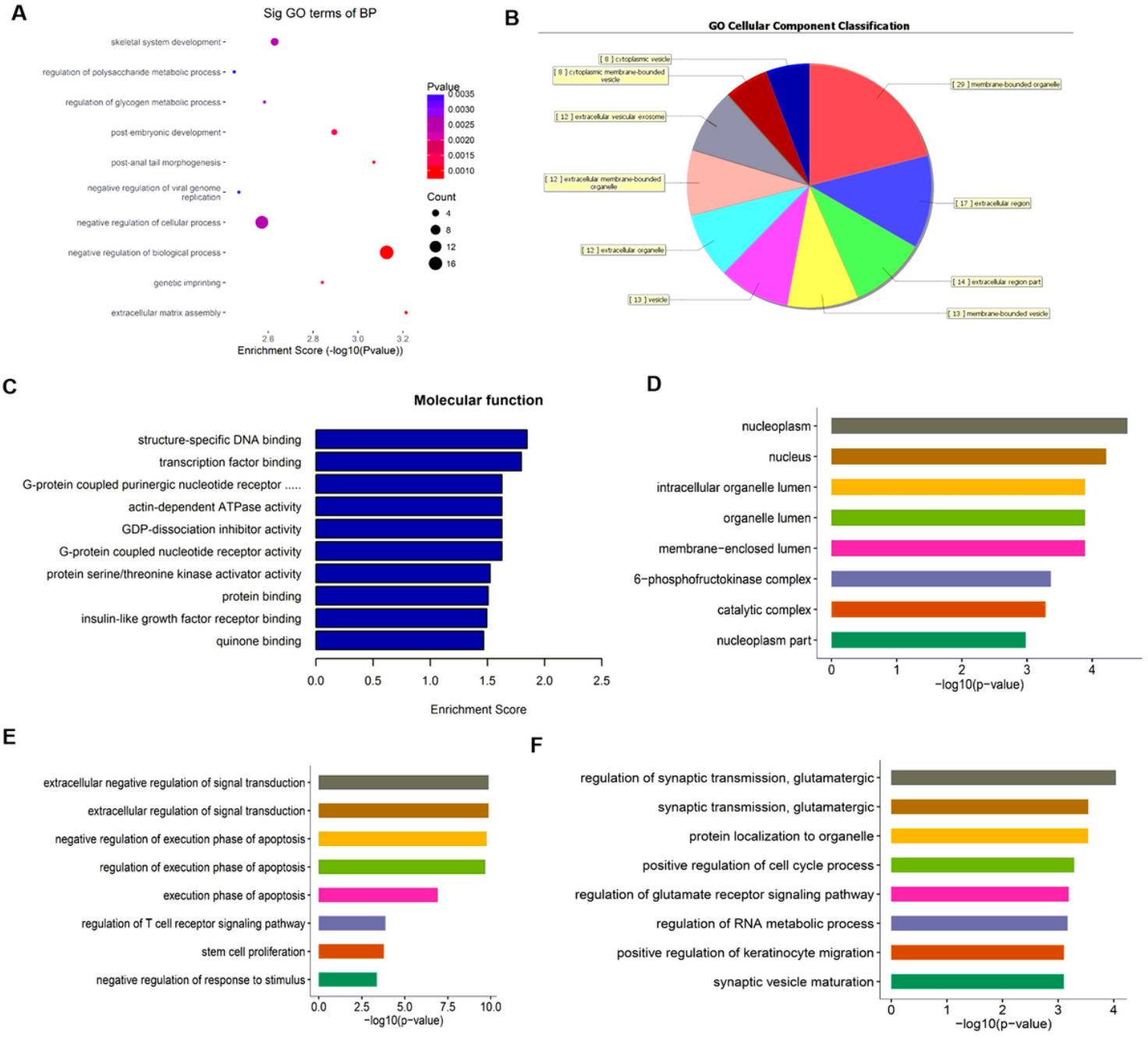

Figure 4

Gene ontology analysis of commonly and specifically methylated genes was conducted between the OLF and control groups. (A) The significant GO terms of BP was presented using bubble diagram. (B) GO cellular component of classification was investigated using pie chart. (C) The molecular function analysis of was performed to investigate the potential mechanism of m6A in OLF. (D-F) GO functional analysis of specifically methylated genes was performed to detect the related molecular mechanism of m6A methylation in OLF.

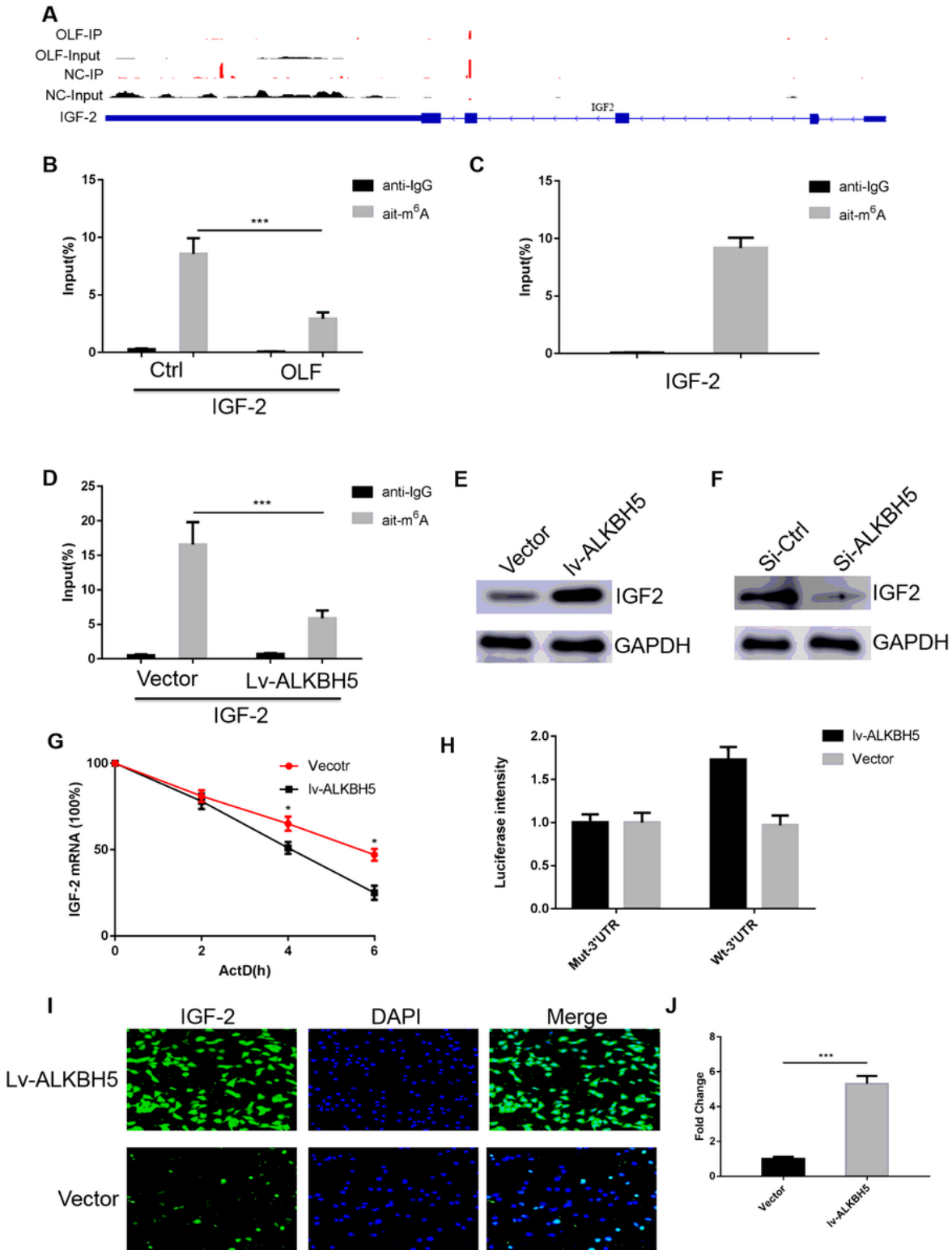

Figure 5

The m6A methylation of IGF-2 in OLF was detected. (A) The m6A methylation of IGF-2 was visualized using MeRIP-seq between the IP and Input group. (B) MeRIP-qPCR was performed to investigate the m6A methylation of IGF-2 between the OLF and control group. (C) The m6A methylation of IGF-2 was detected in normal ligamentum flavu cells. (D) The m6A methylation of IGF-2 was detected when transfected with ALKBH5 overexpression. (E) The expression of IGF-2 was investigated with ALKBH5 overexpression. (F) The expression of IGF-2 was investigated with ALKBH5 knock down. (G) The stability of IGF-2 mRNA was detected using ActD assay. (H) The 3'-UTR of IGF-2 (wild-type and mutant) was cloned and luciferase reporter assay was performed, and these construct was co-transfected with the lv-ALKBH5 or vector into ligamentum flavu cells. (I) Immunofluorescence staining was performed to detect the expression of IGF-2 when transfected with ALKBH5 or vector. (J) The quantitative calculation of immunofluorescence staining using Image J software.

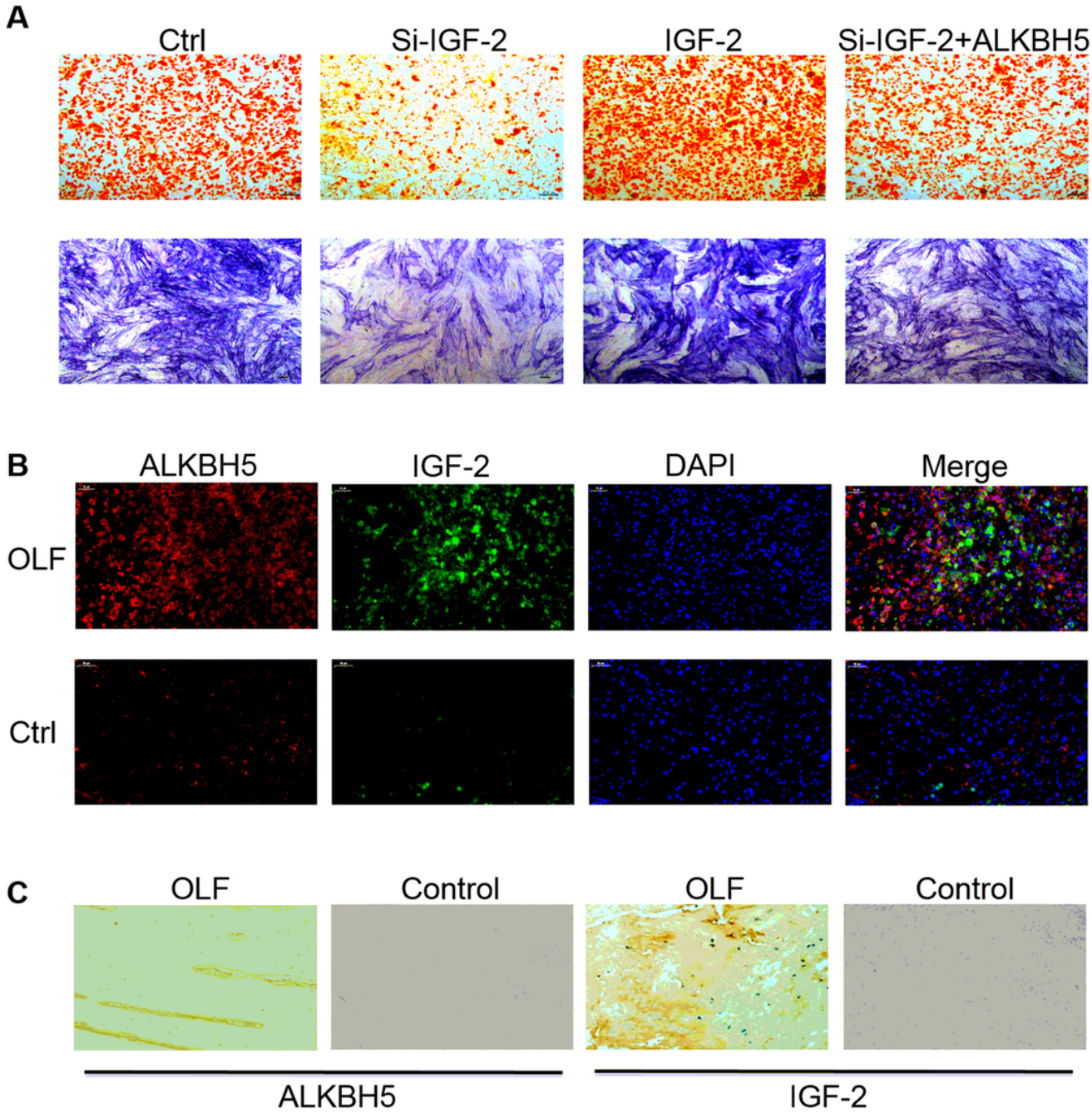

Figure 6

The expression of ALKBH5 and IGF-2 was verified in cell and tissues. (A) The alizarin red staining was performed to investigate the osteogenesis when transfected with si-IGF-2 or si-IGF-2+ALKBH5. (B) The expression of ALKBH5 and IGF-2 was evaluated in OLF and normal tissues. (C) IHC was performed to evaluate the expression of ALKBH5 and IGF-2.